

# Mössbauer spectrometry of $A_2\text{FeMoO}_6$ ( $A = \text{Ca, Sr, Ba}$ ): Search for antiphase domains

J. M. Greneche,<sup>1</sup> M. Venkatesan,<sup>2</sup> R. Suryanarayanan,<sup>3</sup> and J. M. D. Coey<sup>2</sup>

<sup>1</sup>Laboratoire de Physique de L'Etat Condensé UPRESA CNRS 6087, Université du Maine, 72085 Le Mans, France

<sup>2</sup>Physics Department, Trinity College, Dublin 2, Ireland

<sup>3</sup>Laboratoire de Physico-Chimie de l'Etat Solide CNRS, UMR 8648, Bat. 414, Université Paris-Sud, 91405 Orsay, France

(Received 18 August 2000; revised manuscript received 7 November 2000; published 29 March 2001)

Mössbauer spectrometry was carried out in the range of temperature from 4 K to well above the Curie temperature on polycrystalline ceramics of  $A_2\text{FeMoO}_6$  ( $A = \text{Ca, Sr, Ba}$ ). A secondary component in all the paramagnetic or ferromagnetic spectra is attributed to iron in the vicinity of a defect in the NaCl-type cation order. The secondary component and the lack of saturation of the magnetization at the half metallic value of  $4 \mu_B$ /formula unit are explained in terms of antisite defects (point defects) and antiphase boundaries (planar defects). The point defects predominate in all three compounds, but there is some evidence of antiphase boundaries from the spectrum of the Ca compound in a 6 T applied field. The dimensions of the antiphase domains are estimated to be of order  $0.5 \mu\text{m}$ . The electronic configuration of iron in the Ca and Sr compounds is close to  $3d^{5.2}$ , whereas it is  $3d^{5.5}$  in the Ba compound.

DOI: 10.1103/PhysRevB.63.174403

PACS number(s): 76.80.+y, 75.50.Gg, 75.60.-d, 75.25.+z

## I. INTRODUCTION

The double perovskites  $A_2BB'O_6$  have two different  $B$ -site cations which tend to order in a NaCl-type superlattice structure, doubling the elementary perovskite cell.<sup>1</sup> Compounds where  $A$  is an alkaline earth cation and  $B = \text{Cr, Fe}$ ,  $B' = \text{Mo, W, Re}$ , are ferromagnetic. Interest in the series was revived by the recent report of Kobayashi *et al.* that  $\text{Sr}_2\text{FeMoO}_6$  is a half-metallic ferromagnet<sup>2</sup> with a Curie temperature of about 415 K, significantly higher than for any mixed-valence manganite.<sup>3</sup> The ceramics show appreciable negative magnetoresistance at room temperature.<sup>2,4-6</sup> The calculated electronic structure of  $\text{Sr}_2\text{FeMoO}_6$  is reminiscent of that of the  $B$ -site cations in  $\text{Fe}_3\text{O}_4$ ; the five  $3d^\uparrow$  electrons are localized on the iron core while the sixth  $\downarrow$  electron moves in a  $\pi^*$  band of mixed  $3d(\text{Fe})t_{2g}$  and  $4d(\text{Mo})t_{2g}$  character. The spin moment for such a half-metallic electronic structure should be exactly  $4 \mu_B$ /formula unit.

Magnetization measurements on bulk samples of the  $A_2\text{FeMoO}_6$  compounds have consistently yielded low-temperature moments which are less than  $4.0 \mu_B$ . Typical values range from  $3.0$  to  $3.9 \mu_B$ .<sup>4,5</sup> Furthermore, neutron diffraction measurements have yielded iron moments of around  $4.0 \mu_B$  with a moment of a few tenths of a Bohr magneton on the Mo site.<sup>7-9</sup>

Here, we present a detailed  $^{57}\text{Fe}$  Mössbauer study of the  $A_2\text{FeMoO}_6$  compounds. The Mössbauer technique is very useful for distinguishing localized and delocalized iron states, and for probing the influence of the cation environment around Fe nuclei. A model is developed which reconciles the magnetization and Mössbauer data in terms of structural defects; single-site disorder<sup>8,10</sup> and antiphase boundaries.<sup>11,12</sup> These defects are illustrated in Fig. 1. Antiphase boundaries arise between two coherent crystallites with different starting sites for the NaCl-type order. They lead to planes of Fe-O-Fe bonds, which are strongly antiferromagnetic. These bonds are absent in the defect-free NaCl structure.

## II. EXPERIMENTAL SECTION

The compounds were synthesized by the standard solid state reaction from a mixture of high purity oxides and carbonates, calcined at  $980^\circ\text{C}$  and then reground and refired, with a final firing at  $1100^\circ\text{C}$  in a mixture of 1%  $\text{H}_2$  in Ar. The crystal structure changes from monoclinic ( $P2_1/n$ ) for Ca, to tetragonal for Sr ( $P4/mmm$ ) and cubic for Ba ( $Fm\bar{3}m$ ). The refined lattice parameters<sup>4</sup> are included in Table II.

Transmission Mössbauer spectrometry was carried out using a  $^{57}\text{Co}(\text{Rh})$  source in the constant acceleration mode. Zero-field Mössbauer spectra have been recorded at different temperatures using either a cryofurnace or a bath cryostat while the in-field Mössbauer spectrum has been obtained at 10 K using a cryomagnetic device where the external field of 6 T is applied parallel to the  $\gamma$  beam. Spectra were analyzed

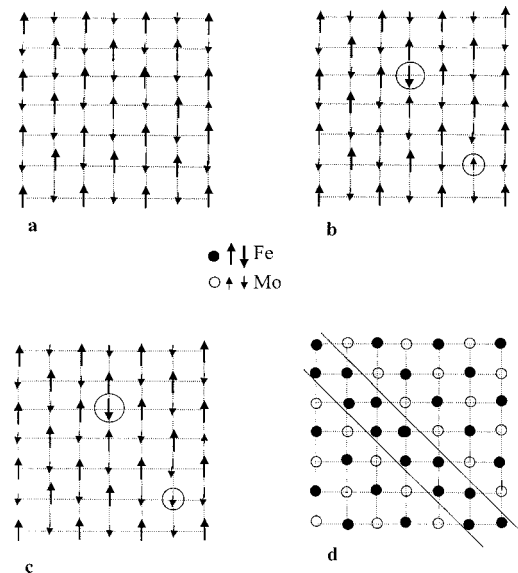


FIG. 1. Schematic illustration of (a) ideal NaCl-type cation order, (b) and (c) antisite defects, and (d) antiphase boundary.

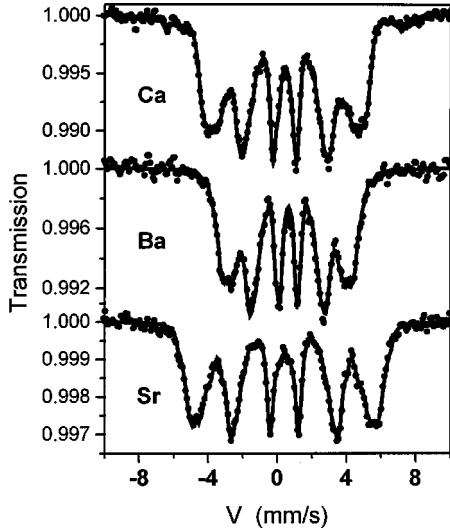


FIG. 2. 300 K Mössbauer spectra recorded on  $\text{Ca}_2\text{FeMoO}_6$ ,  $\text{Ba}_2\text{FeMoO}_6$ , and  $\text{Sr}_2\text{FeMoO}_6$  powders.

by means of a least-squares program MOSFIT<sup>13</sup> and the isomer shift values are quoted relative to that of metallic  $\alpha$ -Fe at 300 K.

### III. RESULTS AND DISCUSSION

#### A. Zero-field $^{57}\text{Fe}$ Mössbauer spectrometry

Room temperature spectra obtained on  $\text{Ca}_2\text{FeMoO}_6$ ,  $\text{Ba}_2\text{FeMoO}_6$ , and  $\text{Sr}_2\text{FeMoO}_6$  powders are compared in Fig. 2: they exhibit magnetic hyperfine structures with broad lines, reflecting both some cationic disorder around Fe nuclei and the proximity of the Curie temperature. These spectra were fitted by means of a discrete distribution of hyperfine

fields linearly correlated to a distribution of isomer shift necessary to describe the small asymmetry of the sextets. The main hyperfine parameters are listed in Table I. One clearly observes that the mean isomer shift value is anomalously high compared to that of common ferric oxides (one expects 0.35–0.40 mm/s). At 77 and 4.2 K, the magnetic spectra are well resolved but show an asymmetrical magnetic hyperfine structure with weakly broadened lines, as shown in Fig. 3. Consequently, two or three sextets are required to describe the magnetic hyperfine structure but the lack of resolution makes it difficult to estimate the proportions of each component accurately. In contrast with low temperature spectra, the spectra taken above the Curie temperature in the paramagnetic state exhibit quadrupolar hyperfine structures which allow the proportions of each iron species to be estimated precisely. These spectra are shown in Fig. 4. The compounds  $\text{Ba}_2\text{FeMoO}_6$  and  $\text{Sr}_2\text{FeMoO}_6$  exhibit an asymmetrical single line whereas  $\text{Ca}_2\text{FeMoO}_6$  shows an asymmetrical quadrupolar doublet. All were fitted with two quadrupolar components characterized by two different isomer shift values, in agreement with low temperature and room temperature results. Hyperfine data are included in Table I. The main component of spectra of the Ba and Sr compounds has a low electric field gradient while that of Ca compound is quite large. This can be explained in terms of a local symmetry which is close to cubic in the first two cases, but significantly distorted in the case of Ca, which is the smallest of the A site cations.<sup>7</sup> The high temperature Mössbauer refinement permits us to refit the low temperature spectra (4.2 and 77 K), keeping similar differences between the two isomer shift values and similar proportions of the components (assuming the same recoilless fractions for the iron sites). The refined 4.2 K values are included in Table I.

TABLE I. Hyperfine characteristics of  $\text{Ca}_2\text{FeMoO}_6$ ,  $\text{Ba}_2\text{FeMoO}_6$ , and  $\text{Sr}_2\text{FeMoO}_6$  at 4.2 K, 300 K, and above Curie temperature ( $\delta$ : isomer shift value quoted relative to metallic Fe at 300 K;  $2\epsilon$ : quadrupole shift;  $B$ : hyperfine field).

Compound	Temperature (K)	$\langle\delta\rangle$ (mm/s) $\pm 0.02$	$\langle 2\epsilon \rangle$ (mm/s) $\pm 0.02$	$\langle B \rangle$ (T) $\pm 0.5$	% $\pm 2$
$\text{Ca}_2\text{FeMoO}_6$	4.2	0.61	-0.13	48.0	42
		0.75	-0.03	47.6	53
		0.42	-0.44	53.0	5
	300	0.61	0.01	23.2	
	425	0.41	0.44		42
$\text{Sr}_2\text{FeMoO}_6$	4.2	0.51	0.27		58
		0.63	0.04	49.7	32
	300	0.72	-0.02	47.7	68
		0.58	0.00	29.3	
		0.38	0.48		37
$\text{Ba}_2\text{FeMoO}_6$	4.2	0.48	0.09		63
		0.72	0.10	49.7	9
	300	0.87	0.00	46.0	91
		0.75	-0.04	20.6	
		0.56	0.45		12
	0.68	0.11		88	

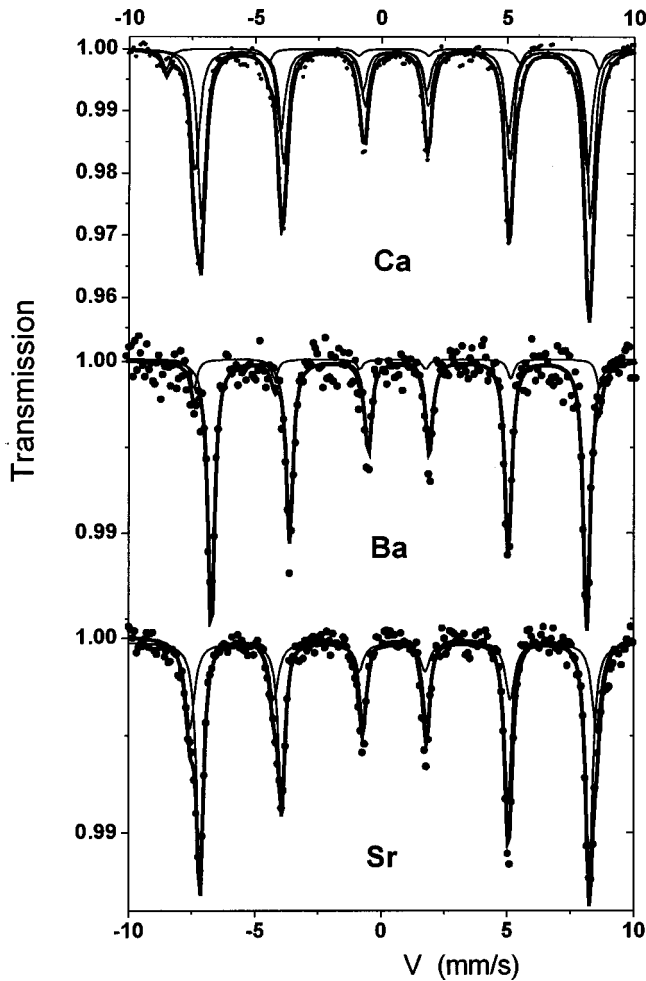


FIG. 3. 4.2 K Mössbauer spectra recorded on  $\text{Ca}_2\text{FeMoO}_6$ ,  $\text{Ba}_2\text{FeMoO}_6$ , and  $\text{Sr}_2\text{FeMoO}_6$  powders.

A spectrum recorded for the Ca sample at 10 K in the 6 T field is illustrated in Fig. 5. One clearly observes a reduction of the magnetic hyperfine splitting and a decrease in intensity of the intermediate lines (labeled 2 and 5). Such features are consistent with most of the Fe moments aligning parallel to the applied field. The Fe hyperfine field is then oriented antiparallel to the applied field, since the prevailing Fermi contribution to the hyperfine field is negative. There is a small component (5% of total area) with an increased hyperfine splitting (58 T). The iron on these sites is aligned antiparallel to the applied field. The fitted parameters are shown in Table II.

Much of the interest in the double perovskites arises from the claim that they are half-metallic. The main objection to this, apart from their rather poor conductivity, is that the low temperature moment is significantly less than the integral value of  $4 \mu_B$ . A stoichiometric half-metal has an integral number of electrons per formula unit, and an integral number in the  $\uparrow$  (or  $\downarrow$ ) band because there is a gap with no  $\downarrow$  (or  $\uparrow$ ) electrons at the Fermi energy. There is therefore an integral number of  $\downarrow$  (or  $\uparrow$ ) electrons, and the difference between the number of  $\uparrow$  and  $\downarrow$  electrons is also an integer. Hence the spin moment is an integral number of Bohr magnetons. For the present compounds this has never been found to the

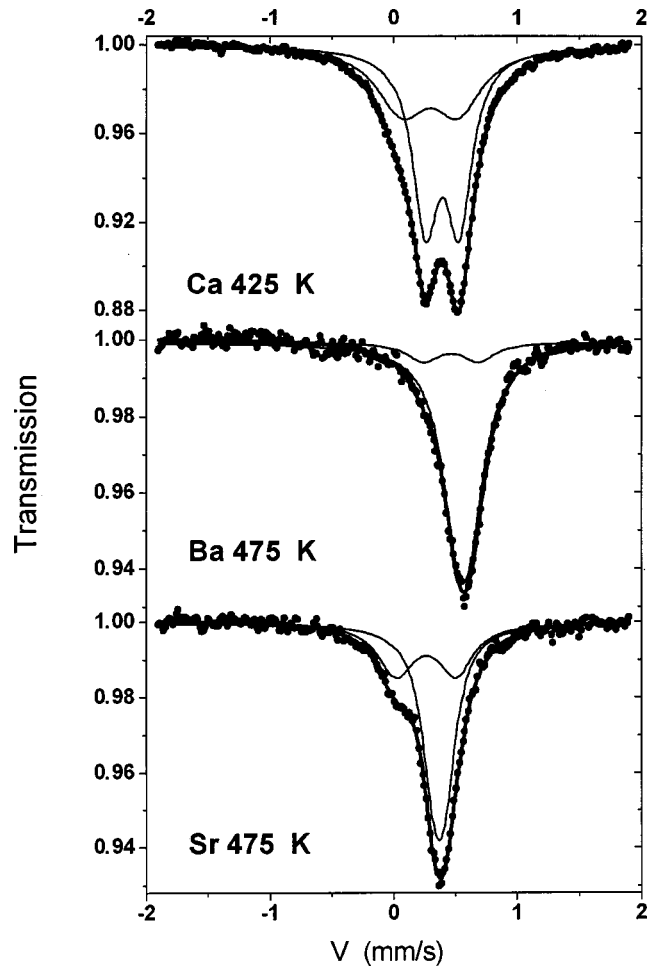


FIG. 4. Paramagnetic Mössbauer spectra recorded on  $\text{Ca}_2\text{FeMoO}_6$ ,  $\text{Ba}_2\text{FeMoO}_6$ , and  $\text{Sr}_2\text{FeMoO}_6$  powders at given temperatures.

case,<sup>4-9</sup> except for thin films.<sup>14</sup> In our samples with  $A = \text{Ca}, \text{Sr},$  and  $\text{Ba}$ , the low-temperature spontaneous magnetization is  $3.63, 3.51,$  and  $3.85 \mu_B/\text{formula unit}$ , respectively.

In a previous study of the Ca compound, we proposed that the secondary component in the Mössbauer spectra should be associated with randomly-disordered iron. If the NaCl-type ordering of Mo and Fe cations is imperfect, and  $p$  is the probability of a cation being on the wrong site then approximately  $6p$  iron ions will see an environment with (5 Mo, 1 Fe) nearest cation neighbors, rather than 6 Mo neighbors, in the ideal structure. Figure 1(b) illustrates this in two dimensions. We would therefore deduce from the intensity of the secondary component listed in Table I that 7, 6, and 2% of the cations are misplaced in the compounds of Ca, Sr, and Ba, respectively. The  $p$  misplaced cations on  $B'$  sites see an environment with (0 Mo, 6 Fe). They will be coupled antiparallel to the  $B$ -site iron sublattice. In the applied field, their hyperfine field will increase. These cations give rise to the small component with a hyperfine field of 58.2 T in the spectrum of Fig. 5. The magnetic moment per formula unit is then  $M = (4 - 8p) \mu_B$  or  $(4 - 10p) \mu_B$  according to whether the misplaced Mo atom has its moment parallel or antiparallel to the majority iron moment [Fig. 1(b) or 1(c)].

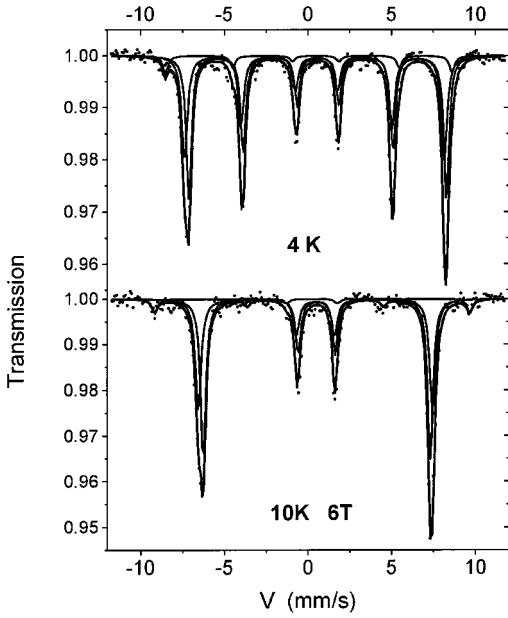


FIG. 5. In-field Mössbauer spectra recorded on  $\text{Ca}_2\text{FeMoO}_6$  powders at 10 K with and without a 6 T field applied parallel to the  $\gamma$  beam.

### B. In-field $^{57}\text{Fe}$ Mössbauer spectrometry

A related model groups the misplaced cations together on antiphase boundaries [Fig. 1(d)] such as exist in thin films of  $\text{Fe}_3\text{O}_4$ ,<sup>15</sup> which show less than the bulk saturation magnetization, and were recently proposed to explain the low magnetization of  $\text{Sr}_2\text{FeMoO}_6$  ceramics<sup>11</sup> and thin films.<sup>12</sup> In polycrystalline materials, nucleation takes place at many points. Normally, the crystallites meet at a grain boundary, but prolonged annealing can lead to grain growth when the antiphase boundaries persist in large crystallites as vestiges of the original grain boundaries. Antiphase boundaries will have consequences for the magnetization of the  $\text{A}_2\text{FeMoO}_6$  series, because the boundaries are planes of Fe-O-Fe superexchange bonds, instead of the normal Fe-O-Mo bonds in the ideal ordered structure. An applied field of order of the exchange field is required to overcome the antiferromagnetic coupling at the antiphase boundary. The problem is similar to that encountered with exchange bias<sup>16</sup> or in the coupling of ferromagnetic and ferrimagnetic films.<sup>17</sup> In an applied field, the regions on either side of the antiphase boundaries are aligned, but there is a quasidomain wall at the boundary which narrows with increasing field. The antiferromagnetically coupled spins at the boundary therefore align perpen-

TABLE II. Hyperfine characteristics of  $\text{Ca}_2\text{FeMoO}_6$  at 10 K under a 6 T applied field ( $\delta$ : isomer shift value quoted relative to metallic Fe at 300 K;  $B_{\text{eff}}$ : effective field;  $B$ : hyperfine field and  $\theta$  the angle between the effective field and the  $\gamma$  beam, i.e., the applied field).

$\delta$ (mm/s)	$B_{\text{eff}}$ (T)	$\theta$ (deg)	$B$ (T)	%
$\pm 0.02$	$\pm 0.5$	$\pm 5$	$\pm 0.5$	$\pm 2$
0.60	42.9	22	48.8	41
0.75	42.1	0	48.1	54
0.41	58.2	0	52.2	5

dicular to the applied field and do not contribute to the magnetization. Furthermore, since they resemble domain walls which are only one atom wide, the antiphase domain boundaries should contribute greatly to the resistance of a half metal in the unmagnetized state. It is possible to reconcile the large resistance of the  $\text{A}_2\text{FeMoO}_6$  compounds with their supposed half-metallicity in this way.

To estimate the maximum number of iron atoms that could be involved in these antiphase boundaries, we make use of the data collected in Table III. An estimate of  $f_5$ , the fraction of iron atoms that do not contribute to the magnetization in 5 T, is  $(4 - M_5)/4$ , where  $M_5$  is the magnetization in 5 T in  $\mu_B/\text{formula unit}$ . We expect this to be roughly twice the number of iron atoms in the antiphase boundary. Based on this idea, the smallest possible size of the antiphase domain,  $d_{ap}$ , is approximately  $12a/f_5$ , where “ $a$ ” is the lattice parameter ( $\sim 0.8$  nm). The lower limit to the antiphase domain size is of order  $0.1 \mu\text{m}$ , which seems plausible, but should be confirmed by electron microscopy.

Unlike an isolated misplaced iron ion, which changes the environment of six others, the iron in an antiphase boundary changes the environment of only two other iron ions. This difference permits a quantitative evaluation of the relative proportions of the two sorts of defects from the intensities of the Mössbauer subspectra. The values of  $p$  deduced from the intensity of the secondary component in the Mössbauer spectra, assuming only antisite defects leads to moments of  $3.44 \mu_B$ ,  $3.52 \mu_B$ , and  $3.84 \mu_B$  for the Ca, Sr, and Ba compounds, respectively, assuming  $M = (4 - 8p) \mu_B$  as expected for the model of Fig. 1(b). The agreement is very good. The alternative hypothesis of only antiphase boundaries is quite inconsistent with the magnetization data. The number of such defects would have to be  $3p$  and the magnetization is then approximately  $(4 - 30p)$ , giving  $1.9 \mu_B$ ,  $2.2 \mu_B$ , and  $3.4 \mu_B$  for the Ca, Sr, and Ba compounds, respectively. The

TABLE III. Set of physical characteristics of the  $\text{Ca}_2\text{FeMoO}_6$ ,  $\text{Sr}_2\text{FeMoO}_6$ , and  $\text{Ba}_2\text{FeMoO}_6$  compounds. ( $\langle\delta\rangle$  is the average isomer shift at 4.2 K.)

Compound	$r_{(A)}$ (nm)	$\langle m \rangle$ $\mu_B/\text{fu}$	$p$ (%)	$(4 - 8p)$ $\mu_B/\text{fu}$	$f_5$ (%)	$d_{ap}(=12a/f_5)$ (nm)	$\langle\delta\rangle$ $\text{mm s}^{-1}$	Fe-O-Fe		
								$3d^n$	(deg) Ref. 7	$d_{B-O}$ (nm)
$\text{Ca}_2\text{FeMoO}_6$	0.106	3.63	7	3.44	8.8	110	0.69	5.24	153	0.199
$\text{Sr}_2\text{FeMoO}_6$	0.127	3.51	6	3.52	12.0	80	0.69	5.25	175	0.198
$\text{Ba}_2\text{FeMoO}_6$	0.143	3.85	2	3.84	3.5	275	0.85	5.49	180	0.200



conclusion that point defects predominate is confirmed by the Mössbauer studies of the Ca compound as shown in Fig. 5. Making the simplified assumption that all iron spins in 6 T are either parallel or perpendicular to the applied field, the percentage of iron atoms that are aligned perpendicular to the field in antiphase boundaries is only 2–3%. From this value, we estimate the size of the antiphase domain to be  $\sim 0.5 \mu\text{m}$ .

Turning now to the question of the iron charge state, it is noteworthy that the iron isomer shift is (i) smaller for the minority site and (ii) the average value correlates with the electronegativity of the A-site cation. The average Fe-O-Mo bond angles and Fe/Mo-O bond lengths are included in the Table III.<sup>7</sup> The width of the  $\pi^*$  band decreases with decreasing bond angle and increasing bond length.

The interpretation of the isomer shift, which is consistent with those reported in related compounds,<sup>18,19</sup> is that the iron charge configuration is modified from purely  $\text{Fe}^{3+}$  by the presence of the  $\pi^*$  electrons. Low temperature values of  $\delta$  for  $\text{Fe}^{3+}$  in oxides are typically 0.50–0.54  $\text{mm s}^{-1}$ . Taking a value of 0.52  $\text{mm/s}$  for  $\text{Fe}^{3+}$  and 1.20  $\text{mm/s}$  for  $\text{Fe}^{2+}$ , as in  $\text{Sr}_2\text{FeWO}_6$ ,<sup>20</sup> we deduce that Ca and Sr compounds have approximately 0.25 extra  $3d$  electrons on the iron, whereas the Ba compound, which has the lowest hyperfine field has an extra 0.5 electrons. There the iron configuration is approximately  $\text{Fe}^{2.5}$ . The  $\text{Fe}^{2.5}$  charge state recently inferred by Linden *et al.*<sup>21</sup> for the Sr compound results from assuming an extremely low value (0.78  $\text{mm/s}$ ) for the  $\text{Fe}^{2+}$  isomer shift, instead of the value measured in Ref. 20.

#### IV. CONCLUSION

The second component in the  $^{57}\text{Fe}$  Mössbauer spectra, the lack of saturation of the magnetization at the half-metallic value of  $4 \mu_B$  per formula unit and the broadening of the ferromagnetic transition at  $T_C$  in the three double perovskites  $A_2\text{FeMoO}_6$  ( $A = \text{Ca}, \text{Sr}, \text{Ba}$ ) are all explained in a model where 2–8% of the iron ions are misplaced from the ideal NaCl type order. The misplaced atoms mostly form random defects but there is evidence that a few of them associate on antiphase domain boundaries. The dimensions of the antiphase domains is expected to be of order  $0.5 \mu\text{m}$ . They should be sought by high resolution electron microscopy. The electronic structure of the iron is not exactly  $3d^5$  because of the partial  $3d(\text{Fe})$  character of the  $\downarrow$  electrons in the  $\pi^*$  band made up of  $3d(\text{Fe})t_{2g}$  and  $4d(\text{Mo})t_{2g}$  electrons. The electronic configuration of iron in the Sr and Ca compounds is close to  $3d^{5.2}$ , whereas that in the Ba compound is approximately  $3d^{5.5}$ .

#### ACKNOWLEDGMENTS

This work was supported by the EU as part of the Oxide Spin Electronics Network (OXSEN) and it forms part of the work included in the AMORE project.

- 
- <sup>1</sup>M. T. Anderson, K. B. Greenwood, G. A. Taylor, and K. R. Poeppelmeier, *Prog. Solid State Chem.* **22**, 197 (1993).
- <sup>2</sup>K. I. Kobayashi, T. Kimura, H. Sawada, K. Terakura, and Y. Tokura, *Nature (London)* **395**, 677 (1998).
- <sup>3</sup>J. M. D. Coey, M. Viret, and S. von Molnar, *Adv. Phys.* **48**, 167 (1999).
- <sup>4</sup>R. P. Borges, R. M. Thomas, C. Cullinan, J. M. D. Coey, R. Suryanarayanan, L. Ben-Dor, L. Pinsard-Gaudart, and A. Revcolevschi, *J. Phys. Condens. Matter* **11**, L445 (1999).
- <sup>5</sup>T. H. Kim, M. Uehara, S. W. Cheong, and S. Lee, *Appl. Phys. Lett.* **74**, 1737 (1999).
- <sup>6</sup>T. Manako, M. Izumi, Y. Konishi, K. I. Kobayashi, M. Kawasaki, and Y. Tokura, *Appl. Phys. Lett.* **74**, 2215 (1999).
- <sup>7</sup>C. Ritter, M. R. Ibarra, L. Morellon, J. Blasco, J. Garcia, and J. M. De Teresa, *J. Phys.: Condens. Matter* **12**, 8295 (2000).
- <sup>8</sup>L. Pinsard-Gaudart, R. Suryanarayanan, A. Revcolevschi, J. Rodriguez-Carvajal, J.-M. Greneche, P. A. I. Smith, R. M. Thomas, R. P. Borges, and J. M. D. Coey, *J. Appl. Phys.* **87**, 7118 (2000).
- <sup>9</sup>B. García-Landa, C. Ritter, M. R. Ibarra, J. Blasco, P. A. Algarabel, R. Mahendiran, J. Garcia, *Solid State Commun.* **110**, 435 (1999).
- <sup>10</sup>A. S. Ogale, S. B. Ogale, R. Ramesh, and T. Venkatesan, *Appl. Phys. Lett.* **75**, 537 (1999).
- <sup>11</sup>J. B. Goodenough and R. I. Dass, *Int. J. Inorg. Mater.* **2**, 3 (2000).
- <sup>12</sup>H. Q. Yin, J. S. Zhou, R. Dass, J. P. Zhou, J. T. McDevitt, and J. B. Goodenough, *J. Appl. Phys.* **87**, 6761 (2000).
- <sup>13</sup>J. Teillet and F. Varret, MOSFIT program, University du Maine (unpublished).
- <sup>14</sup>W. Westerburg, D. Reisinger, and G. Jakob, *Phys. Rev. B* **62**, R767 (2000).
- <sup>15</sup>M. L. Rudee, D. T. Margulies, and A. E. Berkowitz, *Microsc. Microanal.* **3**, 126 (1997).
- <sup>16</sup>A. E. Berkowitz and K. Takano, *J. Magn. Magn. Mater.* **200**, 552 (1999).
- <sup>17</sup>J. E. Wegrowe, A. Comment, Y. Jaccard, J. P. Ansermet, N. M. Dempsey, and J. P. Nozieres, *Phys. Rev. B* **61**, 12 216 (2000).
- <sup>18</sup>A. W. Sleight and J. F. Weither, *J. Phys. Chem. Solids* **33**, 679 (1972).
- <sup>19</sup>M. Abe, T. Nakagawa, and S. Nomura, *J. Phys. Soc. Jpn.* **35**, 1360 (1973).
- <sup>20</sup>H. Kawanaka, I. Hase, S. Toyama, and Y. Nishihara, *J. Phys. Soc. Jpn.* **68**, 2890 (1999).
- <sup>21</sup>J. Lindén, T. Yamamoto, M. Karppinen, H. Yamauchi, and T. Pietart, *Appl. Phys. Lett.* **76**, 2925 (2000).